Inflammopharmacology (2021) 29:1487–1501
https://doi.org/10.1007/s10787-021-00873-0

Inflammopharmacology

ORIGINAL ARTICLE

The role of dorsal root ganglia alpha-7 nicotinic acetylcholine receptor in complete Freund's adjuvant-induced chronic inflammatory pain

Xiaoyu Zhang[1,2,3] · Fangxia Xu[1] · Lijuan Wang[1] · Jinbao Li[1] · Jianhai Zhang[1] · Lina Huang[1]

Received: 31 May 2021 / Accepted: 25 August 2021 / Published online: 12 September 2021

Abstract

Background Alpha-7 nicotinic acetylcholine receptor (α7 nAChR) was reported to have a critical role in the regulation of pain sensitivity and neuroinflammation. However, the expression level of α7 nAChR in dorsal root ganglion (DRG) and the underlying neuroinflammatory mechanisms associated with hyperalgesia are still unknown.

Methods In the present study, the expression and mechanism of α7 nAChR in chronic inflammatory pain was investigated using a complete Freund's adjuvant (CFA)-induced chronic inflammatory pain model. Subsequently, a series of assays including immunohistochemistry, western blotting, and quantitative real-time polymerase chain reaction (qRT-PCR) were performed.

Results α7 nAChR was mostly colocalized with NeuN in DRG and upregulated after CFA injection. Microinjection of α7 nAChR siRNA into ipsilateral L4/5 DRGs aggravated the CFA-induced pain hypersensitivity. Intrathecal α7 nAChR agonist GTS-21 attenuated the development of CFA-induced mechanical and temperature-related pain hypersensitivities. In neuronal the SH-SY5Y cell line, the knockdown of α7 nAChRs triggered the upregulation of TRAF6 and NF-κB under CFA-induced inflammatory conditions, while agitation of α7 nAChR suppressed the TRAF6/NF-κB activation. α7 nAChR siRNA also exacerbated the secretion of pro-inflammatory mediators from LPS-induced SH-SY5Y cells. Conversely, α7 nAChR-specific agonist GTS-21 diminished the release of interleukin-1beta (IL-1β), IL-6, IL-8, and tumor necrosis factor-α (TNFα) in SH-SY5Y cells under inflammatory conditions. Mechanistically, the modulation of pain sensitivity and neuroinflammatory action of α7 nAChR may be mediated by the TRAF6/NF-κB signaling pathway.

Conclusions The findings of this study suggest that α7 nAChR may be potentially utilized as a therapeutic target for therapeutics of chronic inflammatory pain.

Keywords α7 nAChR · Dorsal root ganglion (DRG) · Inflammatory pain · TRAF6 · NF-κB

Introduction

Chronic pain is a debilitating and complex public health issue that affects approximately 20% (120 million) of the global population and gives rise to approximately 10% (60 million) new cases every year (van Hecke et al. 2014; Ruan and Kaye 2016). Healthcare expenses and decrease in productivity due to chronic pain have been estimated at billions of dollars each year (Pasquale et al. 2014; DeBar et al. 2018). Inflammatory pain is commonly caused by thermal, chemical, mechanical injuries, or inflammatory mediators in the nervous system (Ghasemlou et al. 2015). Currently available treatment regimens for chronic inflammatory pain include non-steroidal anti-inflammatory drugs (NSAIDs) and opioids, among other less popular therapies; however, their use has been limited because of severe adverse effects as well as poor efficacy (Baron et al.

✉ Jianhai Zhang
jay8175@163.com

✉ Lina Huang
honilla@163.com

[1] Department of Anesthesiology, Shanghai General Hospital, School of Medicine, Shanghai Jiaotong University, Shanghai 200080, China

[2] Department of Anesthesiology, International Peace Maternity and Child Health Hospital, School of Medicine, Shanghai Jiaotong University, Shanghai 200030, China

[3] Shanghai Key Laboratory of Embryo Original Diseases, Shanghai 200030, China

2018; Busse et al. 2018). Although various cellular and molecular mechanisms have been revealed in the process of inflammatory pain, the related concerns are ineffectively managed by physicians (Müller-Schwefe et al. 2017). Consequently, novel and safe analgesic agents against inflammatory pain are required imminently.

Alpha-7 nicotinic acetylcholine receptors (α7 nAChR) are commonly expressed in the nervous system and are localized to neuronal and non-neuronal cells (Sabec et al. 2018; Licheri et al. 2018). In neurons, it is considered that α7 nAChR plays a critical role in synaptic plasticity, contributing to dependence, learning, memory, and other cognitive functions (Criscuolo et al. 2015; Shenkarev et al. 2020). The activation of α7 nAChR can also contribute to calcium influx, neuronal excitability, neurotransmitter release, and other cellular activities (Licheri et al. 2018). Currently, 11 nAChR neuronal subunits have been identified, including α7 nAChR, which is considered to be a promising therapeutic target for some neurological diseases involving anti-inflammatory as well as antinociceptive effects (Kalkman and Feuerbach 2016; Donvito et al. 2017). Recent studies have shown that the activation of α7 nAChR inhibits the release of inflammatory cytokines as well as alleviating inflammatory pain (Godin et al. 2019; Sun et al. 2019). The α7 nAChR exhibits an ionotropic/metabotropic role during anti-inflammatory signaling mechanisms (Chrestia et al. 2021). Moreover, pharmacological and genetic studies have demonstrated that α7 nAChR has an important role in the regulation of inflammatory pain in several animal models (Bagdas et al. 2016, 2018). The dorsal root ganglions (DRG) acts a central component in signal transmission from the peripheral nervous system towards the central nervous system. Recent studies have suggested that inflammatory mediators can change the activation and function of DRG receptors (Stötzner et al. 2018; Liang et al. 2013). Despite the evidence showing the analgesic effect of the nAChR pathway, the content and distribution of α7 nAChR in DRG and the related mechanisms underlying the inflammatory pain remain unclear.

In this study, we initially assessed the distribution and expression of α7 nAChR in the DRG after the development of inflammatory pain using complete Freund's adjuvant (CFA). Subsequently, we examined the effects of altered α7 nAChR expression levels in the DRG on the generation and persistence of chronic inflammatory pain. Finally, the potential α7 nAChR-associated mechanisms involved in inflammatory pain were investigated.

Materials and methods

Experimental animals

All animal experimental procedures used in this study were approved by the Laboratory Animal Ethics Committee of International Peace Maternity and Child Health Hospital (Shanghai, China) and complied with the International Association for the Study of Pain. Eight-week-old adult male C57BL/6 mice were obtained from the Shanghai Laboratory Animal Corporation (SLAC, Shanghai, China) and maintained on a 12-h light/dark cycle with ad libitum access to rodent chow and water. The environment was maintained at constant temperature (24 °C) and relative humidity (50–60%). All focal animals were acclimated to laboratory conditions for 1 week prior to behavioral tests to minimize the inter- and intra-individual variability of behavioral outcomes. The experimenters who conducted behavioral measurements were blinded to the treatment conditions.

Induction of inflammatory pain

A CFA-induced inflammatory pain model was carried out following a method described previously by Matsuoka et al. (2019). First, mice were briefly exposed to 2–3% sevoflurane; then, 20 µL of undiluted CFA (Sigma) was administered into the plantar surface of the left hind paw using a 28-gauge needle with a 1-mL syringe. Similarly, the mice in the sham group were injected with an equivalent volume of normal saline in the same way. After recovering from anesthesia, the animals were maintained at room temperature of 22–24 °C until further experiments were performed 2 h post-CFA injection. In order to detect the effect of CFA-induced inflammatory pain on α7 nAChR protein expression, the mice were randomly allocated into a CFA group and sham group. There were six mice in each group.

Immunofluorescence and microscopy

As detailed previously (Zhao et al. 2017), we anesthetized the mice using sevoflurane and performed intracardial perfusion with 0.01 M phosphate-buffered saline (PBS, pH 7.4), and then with 4% paraformaldehyde in 0.01 M PBS. Later, L4/5 DRG tissues were collected and then fixed in 4% paraformaldehyde. The DRG samples were then dehydrated using 30% sucrose, frozen, and sectioned into 10-µm-thick slices. These sections were incubated overnight at 4 °C with primary anti-α7 nAChR (1:500; Bioss) and one of the following primary antibodies as required: anti-NeuN (1:2000; EMD Millipore), anti-glial fibrillary acidic protein (GFAP, 1:2000; Sigma), anti-allograft inflammatory factor 1 (Iba-1, 1:500; Servicebio), anti-neurofilament-200 (NF200, 1:200, Sigma), isolectin B4 (IB4, 1:200, Vector laboratories), and mouse anti-calcitonin gene-related peptide (CGRP, 1:200, Abcam) after blocking for 1 h at room temperature in 10% donkey serum with 0.3% Triton X-100. Later, the samples were subjected to double immunofluorescence staining using a mixture of corresponding secondary antibodies by incubating at room temperature for 2 h. The images were

taken using a fluorescence microscope (Leica DMI4000, Germany) that was equipped with a DFC365FX camera (Leica, Germany). The images generated by immunohistochemistry were quantified with NIH Image J software, $n = 3$ rats per experimental group, $n = 4$–6 sections ganglia per animal. An average percentage relative to the total number of neurons was obtained for each animal across the different tissue slides, and then the mean ± SE across animals was determined.

Behavioral tests and drug administration

As earlier described, two calibrated von Frey filaments (weights of 0.07 and 0.4 g, Stoelting Co.) were employed to determine frequency of paw withdrawal in response to mechanical stimuli (Zhao et al. 2017). The mice were individually placed in a transparent glass chamber that was situated on a raised mesh platform and were allowed to adapt to the environment for 60 min. Single strands of the von Frey hair were used to stimulate both hind paws on the plantar sides for approximately 1 s and this procedure was repeated 10 times. A rapid paw withdrawal was considered as a positive response. The following equation was used to calculate the paw withdrawal frequency: paw withdrawal frequency = (number of paw withdrawals/10 trials) × 100%.

The thermal pain test was conducted with a Model 336 Analgesic Meter (IITC Inc.), as previously described (Zhao et al. 2017). Briefly, the mice were placed in clear Plexiglas cases situated on a glass plate. Then, a beam of light was generated by a radiant heat source and aimed at the middle of the plantar surface of every hind paw. When the animal rapidly lifted its foot, we immediately turned off the infrared beam. The duration of the exposure to the beam was regarded as the latency of paw withdrawal. The tests were performed five times at 5-min intervals on each side of animal's hind paws. A cutoff point to avoid tissue damage was set at 20 s.

The cold pain test was conducted by determining the latency to paw withdrawal to cold conductions (0 °C) using a cold metal plate, and the temperature of the aluminum plate was continuously monitored using a thermometer (Zhao et al. 2017). The mice were individually placed in a Plexiglas case located on top of a cold plate. Paw withdrawal latency was defined as the length of time from the placement of the mouse to the mouse jumping. We repeated each trial three times at 15-min intervals. We used a cutoff point to avoid tissue damage of 20 s.

The doses of GTS-21 used in this study were based on the prior study and were adjusted according to the body surface area of mouse as well as different administration mode (Loram et al. 2010). GTS-21 was diluted with saline and injected intrathecally in a total volume of 5 μL before behavioral tests. Control animals were intrathecally injected with an equivalent volume of 0.9% saline. Then, 20,000 nM/mice (5 μL) of GTS-21 was intrathecally injected to assess whether stimulation of DRG α7 nAChR affected CFA-induced hyperalgesia. Different doses of GTS-21 (5000 nM/mice, 10,000 nM/mice, and 20,000 nM/mice) were used for intrathecal injection to estimate whether GTS-21 has a dose-dependent effect.

Intrathecal injection

Direct lumbar puncture was performed as previously described (Maiar et al. 2018). Briefly, a Hamilton syringe with a thin needle was inserted between L5 and L6 vertebrae. The tail reflex is an indication of entry to the subarachnoid space. After injection, the syringe was maintained for 5 s and then rotated and removed, and the locomotion of mice was checked. In order to detect the effect of α7 nAChR agonist on CFA-induced inflammatory pain, the mice were randomly allocated into sham + vehicle group, sham + GTS-21group, CFA + vehicle group, and CFA + vehicle group. There were six mice in each group. In order to detect whether the effects of GTS-21 were dose-dependent, the mice were randomly allocated into sham + vehicle group, CFA + 5000 nM/mice group, CFA + 10,000 nM/mice group, and CFA + 20,000 nM/mice group. There were six mice in each group.

Western blot analysis

Western blot analysis was conducted as described previously (Zhao et al. 2017). The mice were killed after sevoflurane-induced anesthesia. Then, after bilateral L4/5 DRGs were collected, they were frozen in liquid nitrogen. Then, homogenization of the DRGs or cell lines was performed in ice-cold RIPA lysis buffer (Beyotime Biotechnology) that was supplemented with a protease and phosphatase inhibitor cocktail (Beyotime Biotechnology). Later, we collected the clarified supernatants after centrifuging at 15,000 rpm for 15 min at 4 °C. We separated an equivalent of protein using 10% SDS-PAGE and then transferred this to a polyvinylidene difluoride (PVDF) membrane. After being blocked with 5% nonfat milk, the membranes were probed overnight at 4 °C with the following primary antibodies: rabbit anti-α7 nAChR (1:1000; Bioss), rabbit anti-P65 (1:1000; CST), rabbit anti-P-P65 (1:1000; Affinity), rabbit anti-TRAF6 (1:1000; Abcam), rabbit anti-GAPDH (1:5000; Affinity), and rabbit anti-H3 (1:2000; CST). Finally, horseradish peroxidase-conjugated anti-rabbit secondary antibodies (1:5000; BBI) were used to detect the proteins. The immunoreactive signals were detected with an enhanced chemiluminescence (ECL) kit and visualized using ChemiDoc XRS with Image Lab software (Bio-Rad). Band intensities were quantified by densitometry using Image Lab software (Bio-Rad). The

level of the nuclei protein was normalized to total histone H3, whereas the intensity of the other protein bands was normalized to that of GAPDH.

DRG microinjection

As previously described by Zhao et al. (2017), after the mice were anesthetized with sevoflurane, a midline incision was created in the lower lumbar back. Then, the left lumbar articular process was exposed and isolated. Following this, the exposed DRG in an siRNA solution (1–2 μL, 20 mM) was injected at a rate of 50 nL/min using a glass micropipette that was connected to an air pressure system. Subsequently, the glass micropipette was left to stand for 5–10 min and then withdrawn to allow diffusion. Later, the wound was washed using sterile saline, and closure of the skin incision was performed with a 3-0 silk thread. Mice with paresis or other irregularities were removed from subsequent experiments.

α7 nAChR siRNA and the negative control siRNA were purchased from Sangon Biotech. To prevent degeneration and improve the delivery of siRNA, we used Entranster™ in vivo transfection, as described previously (Peng et al. 2017). The siRNA target sequence sense 5′-GCAGUGCAA ACUGAAGUUUTT-3′ and antisense 5′-AAACUUCAG UUUGCACUGCTT-3′ were selected for α7 nAChR. In order to examine whether blocking the increase in α7 nAChR in DRG could aggravate the CFA-induced pain hypersensitivity, the mice were randomly allocated into sham group, sham + negative control (NC) group, CFA + NC group, siRNA + CFA group, and siRNA + sham group. There were six mice in each group.

Cell culture and transfection

Neuronal SH-SY5Y cells were obtained from the Shanghai Institute of Biological Sciences (Shanghai, China). SH-SY5Y cells were cultured in DMEM/high glucose medium (Gibco) supplemented with 10% fetal bovine serum. The cells were kept at 37 °C in a humidified incubator with 5% CO_2. We diluted the α7 nAChR siRNA and negative control siRNA to a concentration of 100 nM and then separately transfected these into SH-SY5Y cells using Lipofectamine 2000 (Invitrogen). After 48 h, the cells were collected for western blotting and quantitative real-time PCR analysis.

Quantitative real-time RT-PCR

mRNA levels were determined by extracting total RNA with RNAiso Plus (TaKaRa) following the manufacture's protocol. Approximately 300 ng of total RNA was used as template for reverse transcription with a HiScript III 1st Strand cDNA Synthesis Kit (Vazyme). Every sample was repeated in triplicate using a total reaction volume of 20 μL, which contained 80 nM of the forward and reverse primers, 10 μL of the ChamQ Universal SYBR qPCR Master Mix (Vazyme), and 12 ng of cDNA. The primer sequences were as follows: *IL-1β*, sense: 5′-GCCAGTGAAATGATGGCT TATT-3′ and antisense: 5′-AGGAGCACTTCATCTGTT TAGG-3′; *IL-6*, sense: 5′-CACTGGTCTTTTGGAGTT TGAG-3′ and antisense: 5′-GGACTTTTGTACTCATCT GCAC-3′; *IL-8*, sense: 5′-AACTGAGAGTGATTGAGA GTGG-3′ and antisense: 5′-ATGAATTCTCAGCCCTCT TCAA-3′; *TNFα*, sense: 5′-TGGCGTGGAGCTGAGAGA TAACC-3′ and antisense: 5′-CGATGCGGCTGATGGTGT GG-3′; *GAPDH*, sense: 5′-CAAGGTCATCCATGACAA CTTTG-3′ and antisense: 5′-GTCCACCACCCTGTTGCT GTAG-3′. The PCR amplification reaction was as follows: 30 s at 95 °C followed by 10 s at 95 °C, and 30 s at 60 °C for 40 cycles. Melt curves were performed on completion of the cycles to determine the amplification specificity, and the results were processed by the software of the Bio-Rad CFX96 instrument.

Statistical analysis

The mice were randomly assigned to different treatment groups. All data are shown as the mean ± SEM after assessment of normality using the Kolmogorov–Smirnov test. A paired or unpaired Student's *t* test and a one- or two-way repeated ANOVA with a post hoc Bonferroni correction were performed to achieve normal distribution data. The Mann–Whitney *U* test was employed for non-parametric data analysis (GraphPad Prism 6.0). Differences with $P < 0.05$ were considered statistically significant.

Results

α7 nAChR localized in DRG neurons but not in astrocytes or microglia

To investigate the correlation between α7 nAChR and inflammatory pain, we first examined the distribution pattern of α7 nAChR in the DRG by double labeling immunofluorescence staining with the markers specific for neurons, astrocytes, and microglia. The results showed that α7 nAChR (red) colocalizes with NeuN (green), a neuronal marker, in the DRG (Fig. 1a). Nevertheless, α7 nAChR did not show a marked overlap staining with either the astrocytic marker GFAP (green) or the microglial marker Iba-1 (green) (Fig. 1b, c). These results suggested that α7 nAChR is involved in inflammatory pain by influencing DRG neuronal activation. Moreover, subpopulation analysis showed that about 42.13% of α7 nAChR-labeled neurons were positive

for NF200 (a marker for medium/large cells and myelinated Ab fibers) (Fig. 1d), 72.86% were positive for calcitonin gene-related peptide (CGRP) (a marker for small peptidergic neurons) (Fig. 1e), and 16.41% were positive for isolectin B4 (IB4) (a marker for small nonpeptidergic neurons) (Fig. 1f). A cross-sectional area analysis of neuronal somata indicated that about 11.79% of α7 nAChR-labeled neurons were small ($< 600\ \mu m^2$), 52.03% were medium (600–1200 μm^2), and 36.18% were large ($> 1200\ \mu m^2$) (Fig. 1g).

The expression of α7 nAChR in DRG was upregulated following CFA injection

The experimental design is shown in Fig. 2a. Consistent with the results of prior studies (Ghasemlou et al. 2015), CFA injection, but not sham surgery, induced mechanical allodynia, thermal and cold hyperalgesia on the ipsilateral side at 2 h and 1, 3, and 7 days after the injection (Fig. 2b–e) (Liang et al. 2013). Immunohistochemistry showed that the number of α7 nAChR-labeled neurons in the CFA group on day 3 after injection increased by 18% ($P < 0.05$) compared with the corresponding sham group (Fig. 2f, g). In accordance with the immunohistochemistry data, western blotting also revealed an increase in α7 nAChR expression levels in the ipsilateral L4/5 DRGs. However, α7 nAChR expression in the CFA group significantly increased from day 1 (1.28-fold higher than that of the sham group; $P < 0.05$) and peaked on day 3 (1.43-fold increase relative to the sham group; $P < 0.05$), which was maintained for at least 7 days (1.35-fold higher that of the sham group; $P < 0.05$; Fig. 2h, i). These findings indicated that α7 nAChR-labeled neurons in DRG respond to the inflammation caused by CFA.

Intrathecal α7 nAChR agonist alleviated CFA-induced inflammatory pain

Next, we examined whether the agitation of DRG α7 nAChR affected CFA-induced hyperalgesia. The experimental design is shown in Fig. 3a. On day 3, after sham treatment or CFA injection, the α7 nAChR agonist GTS-21 or vehicle was injected intrathecally in a total volume of 5 µL. Behavioral tests were carried out 1 day prior to CFA injection, before intrathecal injection, and 15, 30, 45, 60, 90, and 120 min after injection on day 3 post surgery. Similar to previous studies (Ghasemlou et al. 2015), CFA injection, but not sham surgery, resulted in mechanical allodynia, thermal hyperalgesia, and cold allodynia on the ipsilateral side on day 3 (Fig. 3b–d). In addition, paw withdrawal frequency in response to mechanical stimuli markedly increased and paw withdrawal latency in response to thermal stimulation significantly decreased in the CFA plus vehicle group relative to the sham plus vehicle group (Fig. 3b–d). These CFA-induced pain hypersensitivities were attenuated in a time-dependent fashion on the ipsilateral side after intrathecal injection of the CFA mice with GTS-21 (20,000 nM/mice) (Fig. 3b–d). Compared to the CFA plus vehicle mice, we observed that the CFA mice paw withdrawal frequency of the ipsilateral hind paw after mechanical stimulation was reduced at 15, 30, 45, 60, and 90 min post intrathecal injection (Fig. 3b–d). CFA mice paw withdrawal latency in response to thermal stimuli on the ipsilateral hind paw markedly increased at 15, 30, 45, 60, and 90 min post intrathecal injection relative to the associated CFA plus vehicle mice (Fig. 3b–d).

We observed that the effects of GTS-21 were dose-dependent. Compared with the CFA plus vehicle mice, the application of GTS-21 at the dose of 20,000 nM/mice markedly decreased paw withdrawal frequency in response to mechanical stimulation and largely increased paw withdrawal latency to thermal stimuli on the ipsilateral side of CFA mice at 15, 30, 45, and 60 min post intrathecal injection (Fig. 3e–g). However, there were no differences in paw withdrawal responses to mechanical, heat, and cold stimuli between the CFA plus vehicle group and CFA plus GTS-21 (5000 nM/mice) groups (Fig. 3e–g). Intrathecal GTS-21 did not affect locomotor functions or basal paw responses to mechanical, heat, and cold stimuli on the contralateral side (Supplementary Fig. 1).

Blocking increased α7 nAChR in DRG aggravated the CFA-induced pain hypersensitivity

Intrathecal GTS-21 may lack anatomical specificity. To further confirm the role of DRG α7 nAChR in inflammatory pain, we tested whether inhibiting the upregulation of α7 nAChR via microinjection of its siRNA into the ipsilateral DRGs influenced CFA-induced inflammatory pain. The experimental design is shown in Fig. 4a. Consistent with the above observation, CFA significantly increased the paw withdrawal frequencies in response to mechanical stimuli and reduced the paw withdrawal latencies in response to heat and cold stimuli from 2 h to 3 days post-CFA injection as compared to baseline values (Fig. 4b–e). However, the CFA mice that were pre-microinjected with α7 nAChR siRNA exhibited higher paw withdrawal frequencies and reduced paw withdrawal latencies from 2 h to 3 days post-CFA injection into the ipsilateral side relative to the corresponding negative control siRNA-treated CFA mice (Fig. 4b–e). The pre-injection of α7 nAChR siRNA did not change the basal paw responses of the sham mice to mechanical or thermal stimuli (Fig. 4b–e). The effect of microinjection of α7 nAChR siRNA into the L4/5 DRG on the expression of α7 nAChR was verified by immunofluorescence staining. The results showed that L4/5 DRG-positive cells significantly decreased after microinjection of α7 nAChR siRNA (0.51-fold lower than that of the naive group; $P < 0.05$; Fig. 4f, g).

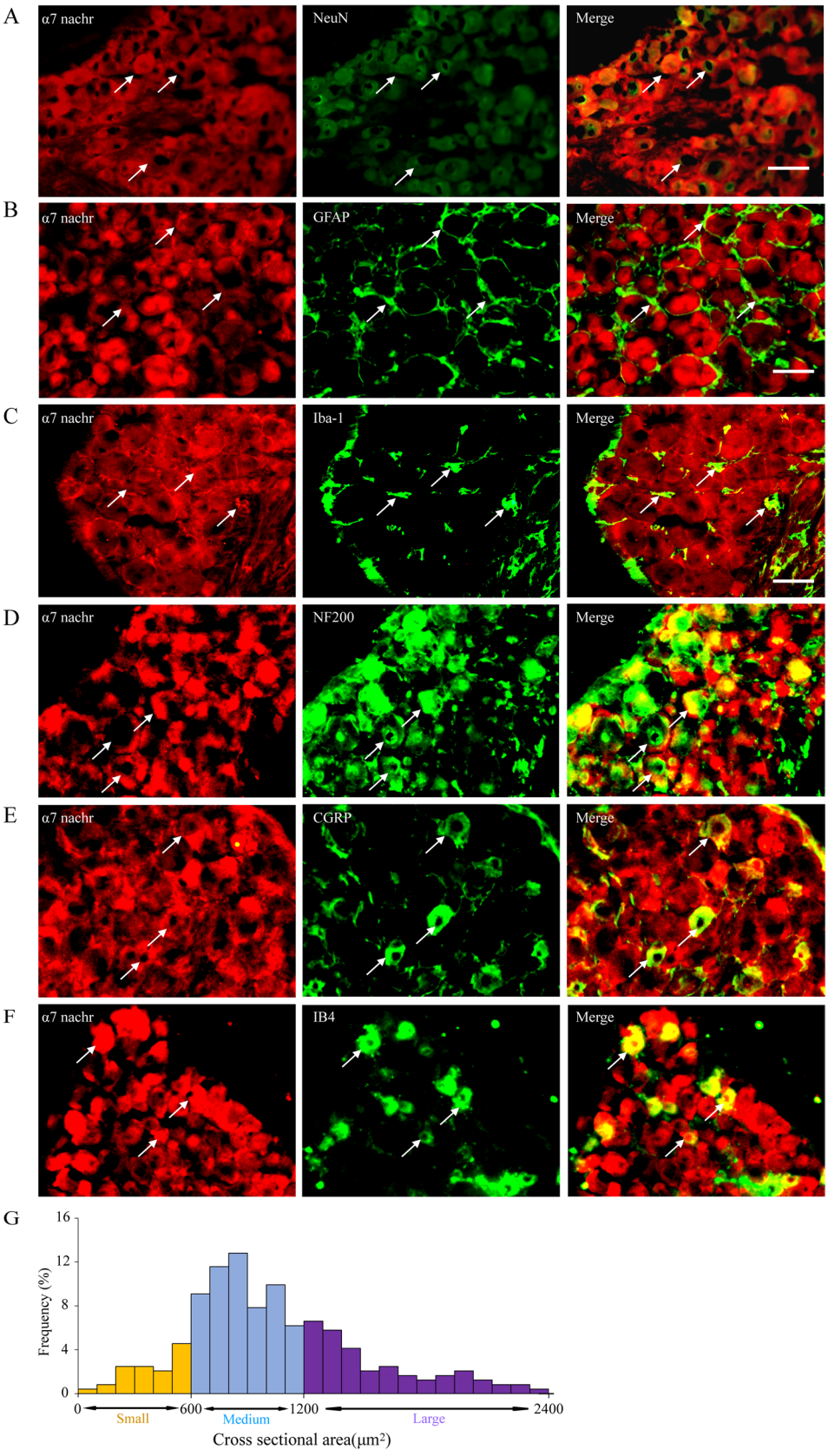

Fig. 1 α7 nAChR is mainly expressed in mouse DRG nociceptive neurons. **a** α7 nAChR was co-localized with NeuN in DRG neurons. **b** α7 nAChR was not co-expressed with GFAP, which stands for astrocytes. **c** α7 nAChR does not exhibit overlapping staining with the microglial marker Iba-1. **d–f** α7 nAChR-positive neurons were labelled by neurofilament-200 (NF200), calcitonin gene-related peptide (CGRP) or isolectin B4 (IB4). **g** Distribution of α7 nAChR-positive somata: small, 11.79%; medium, 52.03%; large, 36.18%

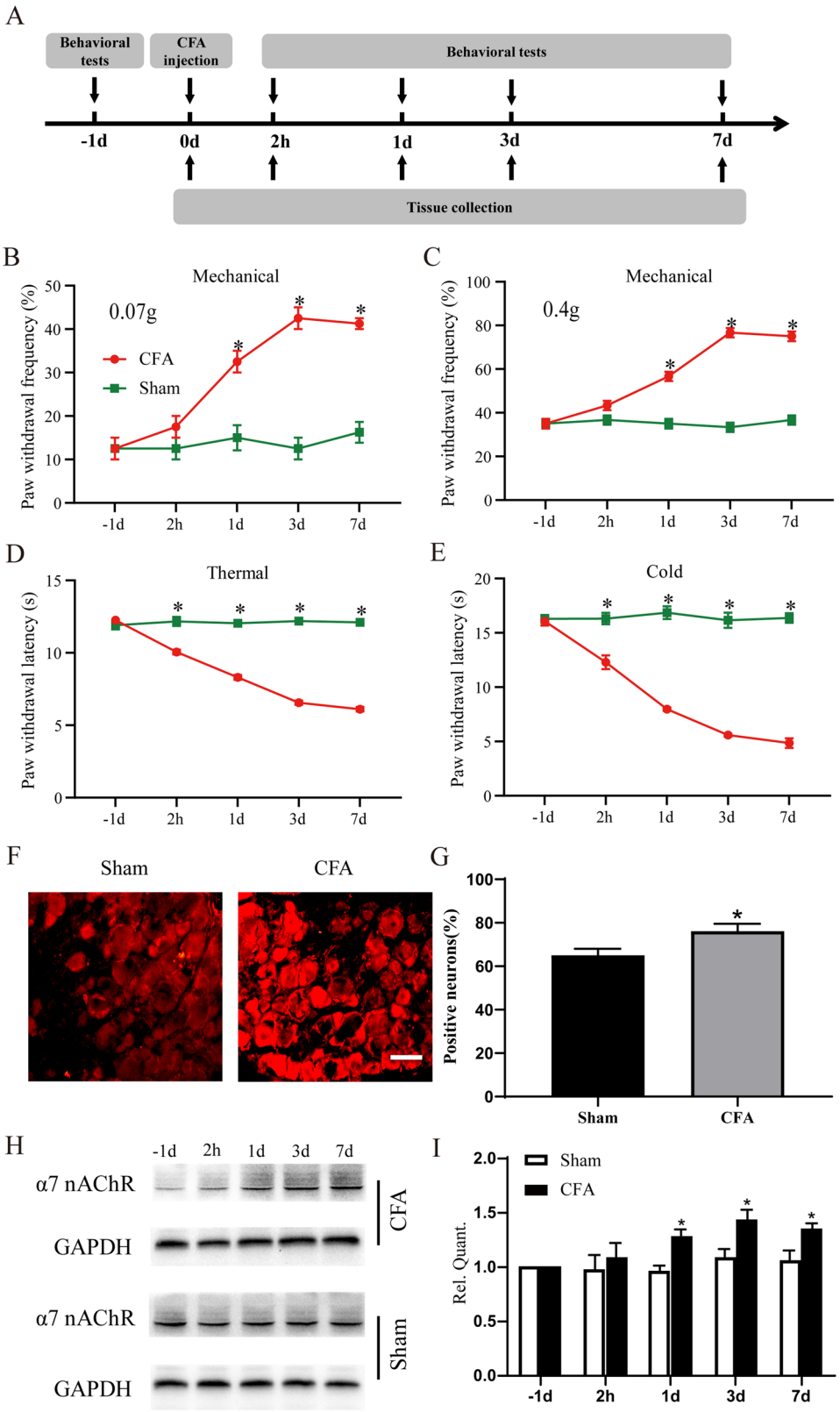

Fig. 2 α7 nAChR expression in the DRG of a CFA-induced inflammatory pain model. **a** Schematic diagram of the experimental procedure. **b**, **c** CFA application results in an increase in paw withdrawal frequency in response to calibrated von Frey hair (0.07 g and 0.4 g) at 2 h, 1, 2, and 7 days post injection. $n=6$ mice/group. Two-way analysis of variance (ANOVA) followed by Bonferroni post hoc test. $^*P<0.05$ vs. sham group. **d**, **e** After CFA injection, paw withdrawal latency in response to thermal stimulation was reduced at 2 h, 1, 3, and 7 days. $n=6$ mice/group. Two-way ANOVA followed by Bonferroni post hoc test. $^*P<0.05$, vs. sham group. **f** Representative images of α7 nAChR-labeled neurons in lumbar DRGs at 7 days after Sham or CFA injection. **g** Immunofluorescence images showed that α7 nAChR-labeled neurons significantly increased after CFA injection. Two-tailed, independent Student's *t* test. $^*P<0.05$ vs. Sham group. **h** Western blotting results showing the expression of the α7 nAChR protein in the mouse ipsilateral L4/5 DRGs after CFA injection at various time points. **i** Intensity analysis revealed that α7 nAChR was significantly upregulated post CFA injection, whereas the sham group did not exhibit any changes in expression from the basal level of α7 nAChR at all time points. Two-way ANOVA followed by Bonferroni post hoc test. $^*P<0.05$, vs. sham group

After completing the behavioral tests, ipsilateral L4/5 DRGs were collected on day 3 post-injection for assessment of α7 nAChR expression. As expected, α7 nAChR protein expression in the ipsilateral L4/5 DRGs on day 3 post CFA injection in mice pre-microinjected with negative control siRNA increased by 1.39-fold compared to sham group

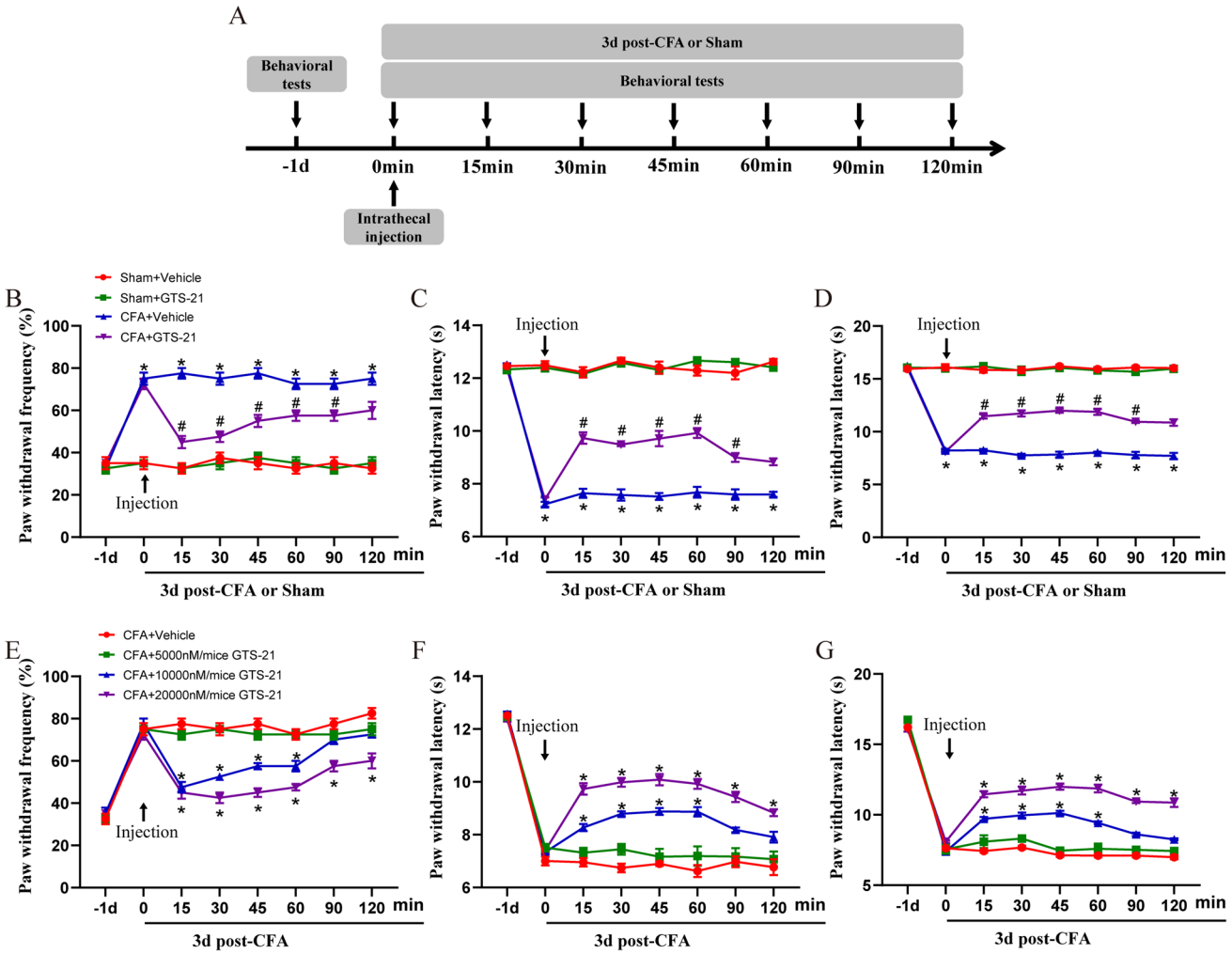

Fig. 3 Effect of GTS-21 intrathecal α7 nAChR agonist on inflammatory pain as induced by CFA. **a** Schematic diagram of the experimental procedure. **b–d** Effect of intrathecal GTS-21 (20,000 nM/mice) or vehicle on paw withdrawal frequencies after application of mechanical stimuli (calibrated von Frey hair 0.4 g), latency of paw withdrawal in response to thermal stimulation 3 days post-CFA injection or sham surgery. $n = 6$ mice/group. Two-way analysis of variance (ANOVA) followed by Bonferroni post hoc test. $^{*}P < 0.05$, sham plus vehicle group, $^{\#}P < 0.05$, vs. the CFA plus vehicle group. **e–g** Dose-dependent effects of intrathecal GTS-21 or vehicle in terms of paw withdrawal frequencies after application of mechanical stimuli (calibrated von Frey hair 0.4 g); paw withdrawal latencies in response to thermal stimulation on day 3 post-CFA injection. $n = 6$ mice/group. Two-way ANOVA followed by Bonferroni post hoc test. $^{*}P < 0.05$, vs. CFA plus vehicle group

that were pre-microinjected with negative control siRNA ($P < 0.05$; Fig. 4g, h). These upregulated expression patterns were not observed in CFA mice that were pre-microinjected with α7 nAChR siRNA (Fig. 4h, i). In addition, we observed a significant decrease in the basal α7 nAChR protein expression levels in the ipsilateral L4/5 DRG of the sham mice that were pre-microinjected with α7 nAChR siRNA (0.49-fold lower than that of the negative control group; $P < 0.05$; Fig. 4g, h).

Effect of LPS on the α7 nAChR expression in neuronal SH-SY5Y cells was dose-dependent

In order to explore the underlying mechanisms, inflammation stimulus was induced by lipopolysaccharide (LPS), and neuronal SH-SY5Y cells were utilized to investigate the downstream pathway of α7 nAChR in inflammatory pain. In addition, we used western blot analysis to detect the level of α7 nAChR protein in neuronal SH-SY5Y cells treated with LPS in a dose-dependent manner and found that α7 nAChR was significantly increased with 0.1 μg/mL LPS treatment for 24 h (1.43-fold that of 0.1 μg/mL LPS group;

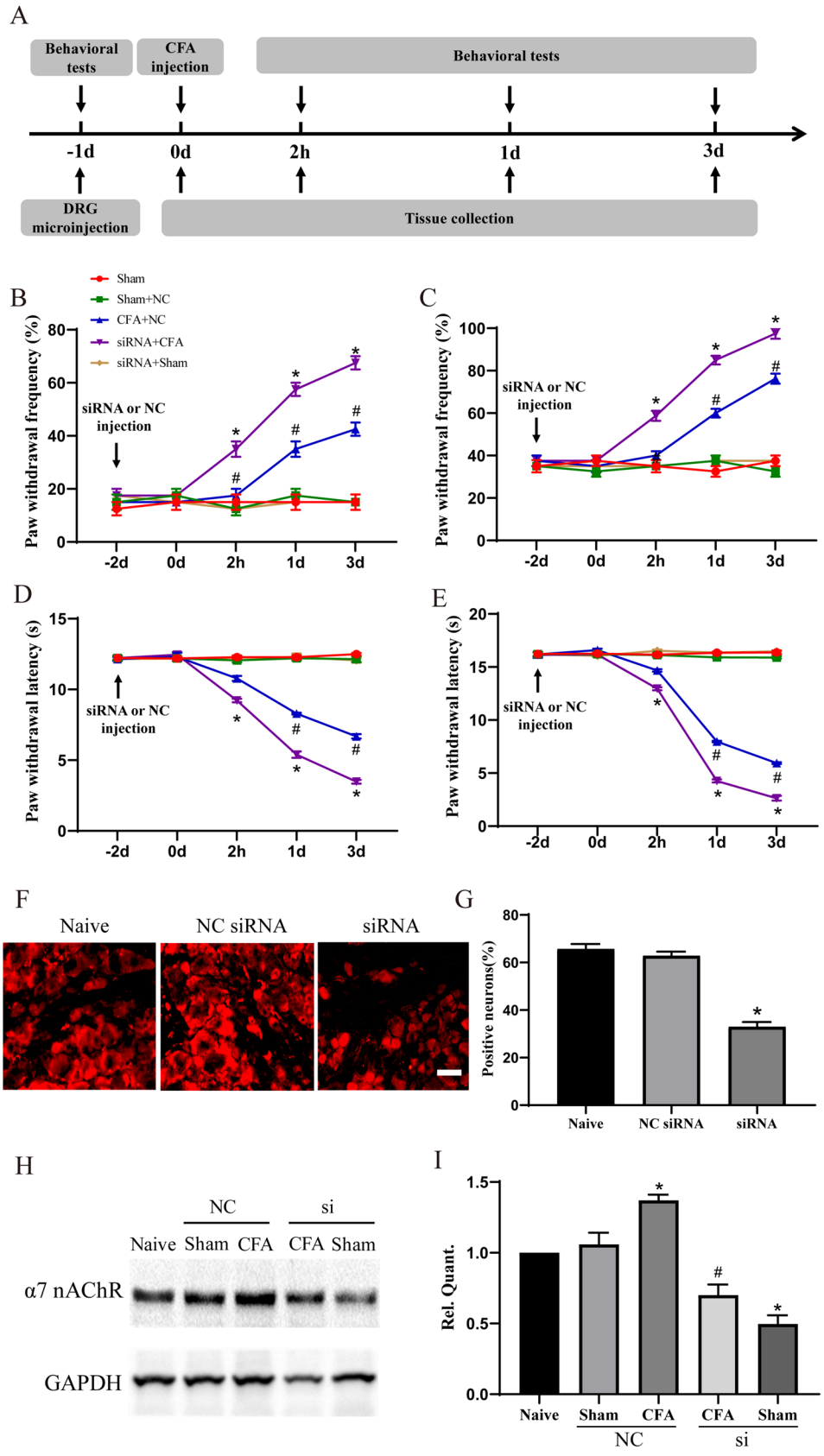

Fig. 4 Effect of α7 nAChR siRNA microinjection on CFA-induced inflammatory pain. **a** Schematic diagram of the experimental procedure. **b**, **c** Effect of α7 nAChR siRNA or NC siRNA microinjection into L4/5 DRG on paw withdrawal frequencies to calibrated von Frey filament (0.07 g and 0.4 g) after CFA injection at different time points. $n = 6$ mice/group. Two-way analysis of variance (ANOVA) followed by Bonferroni post hoc test. $^{*}P < 0.05$, versus sham plus NC group, $^{\#}P < 0.05$, versus CFA plus NC group. **d**, **e** Effect of α7 nAChR siRNA or NC siRNA microinjection into L4/5 DRG on paw withdrawal latencies to heat and cold stimuli after CFA injection at different time points. $n = 6$ mice/group. Two-way ANOVA followed by Bonferroni post hoc test. $^{*}P < 0.05$, versus sham plus NC group, $^{\#}P < 0.05$, versus CFA plus NC group. **f** Representative images of α7 nAChR-labeled neurons in lumbar DRGs after NC siRNA or α7 nAChR siRNA injection. **g** Immunofluorescence images showed that α7 nAChR-labeled neurons significantly decreased after siRNA injection. One-way ANOVA followed by Bonferroni post hoc test. $^{*}P < 0.05$ vs. Sham group. **h**, **i** α7 nAChR protein expression of α7 nAChR siRNA-injected or NC siRNA-injected mice on day 3 after CFA injection. Unilateral L4/5 DRGs were collected together from two mice. $n = 6$–8 mice per group. One-way ANOVA followed by Bonferroni post hoc test. $^{*}P < 0.05$, versus sham plus NC group, $^{\#}P < 0.05$, versus CFA plus NC group

$P < 0.05$; Fig. 5a, b). Therefore, 0.1 μg/mL LPS was used as the optimal concentration.

The TRAF6/NF-κB P65 pathway was triggered by α7 nAChR under inflammatory conditions

Since chronic neuroinflammation induced NF-κB pathway activation and contributed to inflammatory pain, we examined whether knockdown or stimulation of α7 nAChR activated the TRAF6/NF-κB P65 pathway under inflammatory conditions. GTS-21 was used as a specific agonist of α7 nAChR in the subsequent experiments. Consistent with this observation, LPS treatment significantly increased the level of α7 nAChR (1.39-fold that of NC siRNA group; $P < 0.05$; Fig. 6a, b). The transfection of α7 nAChR siRNA significantly knocked down α7 nAChR in SH-SY5Y cells (0.71-fold that of NC siRNA group; $P < 0.05$; Fig. 6a, b). The treatment of LPS-exposed cells with α7 nAChR siRNA partially reversed the upregulation of α7 nAChR as compared to the LPS group (0.81-fold that of the LPS group; $P < 0.05$; Fig. 6a, b). However, no significant alteration was detected in the protein level of p65 subunit with different treatment (Fig. 6a, c). The level of P-P65 and TRAF6 proteins was significantly upregulated after LPS stimulation (P-P65 1.51-fold that of the NC siRNA group; TRAF6 1.25-fold that of the NC siRNA group; $P < 0.05$; Fig. 6a, d, e). In addition, the P-P65 and TRAF6 levels were higher in the LPS with α7 nAChR siRNA group as compared to those in the negative control siRNA (P-P65 1.36-fold that of the LPS group; TRAF6 1.16-fold that of the LPS group; $P < 0.05$; Fig. 6a, d, e). Pre-incubation with 10 μM GTS-21 significantly downregulated the levels of P-P65 and TRAF6 as compared to the LPS group (P-P65 0.61-fold that of the LPS group; TRAF6 0.76-fold that of the LPS group; $P < 0.05$; Fig. 6a, d, e). These results indicated that inhibition of α7 nAChR took part in activating the TRAF6/NF-κB P65 pathway under inflammatory conditions.

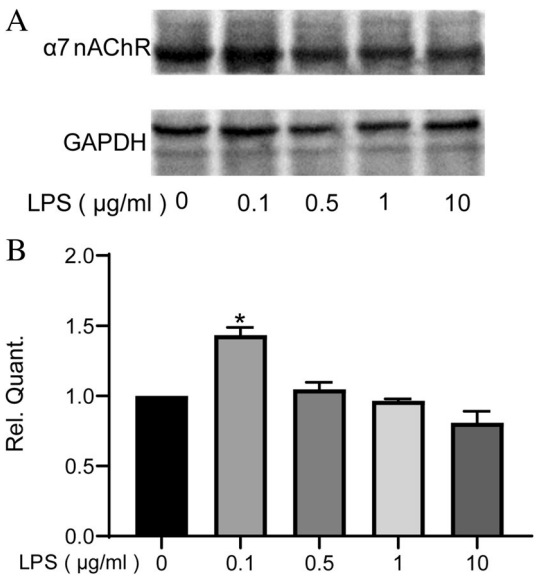

Fig. 5 Dose-dependent effects of LPS on α7 nAChR expression. **a** Western blotting results showing α7 nAChR protein expression in neuronal SH-SY5Y cells after treatment with various concentrations. **b** The results of intensity analysis showing that α7 nAChR expression significantly increased after 0.1 μg/mL LPS treatment for 24 h. One-way analysis of variance (ANOVA) followed by Bonferroni post hoc test. *$P < 0.05$, vs. 0 μg/mL group

α7 nAChR increased the secretion of pro-inflammatory mediators from LPS-induced SH-SY5Y cells

To examine the influence of α7 nAChR on the LPS-induced inflammatory responses of SH-SY5Y cells, the mRNA expressions of interleukin-1β (IL-1β), IL-6, IL-8, and tumor necrosis factor-α (TNFα) were assessed by quantitative real-time RT-PCR and found to be significantly higher after LPS administration than those of the negative control siRNA group (IL-1β 8.92-fold that of the NC group; IL-6 6.68-fold that of the NC group; IL-8 3.41-fold that of the NC group; TNFα 5.14-fold that of the NC group; $P < 0.05$; Fig. 7a–d). Compared to the LPS group, the cotreatment of LPS with α7 nAChR siRNA upregulated the levels of IL-1β, IL-6, IL-8, and TNFα (IL-1β 1.88-fold that of the LSP group; IL-6 1.47-fold that of the LPS group; IL-8 1.90-fold that of the LPS group; TNFα 2.37-fold that of the LPS group; $P < 0.05$; Fig. 7a–d). The coadministration of LPS with 10 μM GTS-21 significantly decreased the levels of IL-1β, IL-6, IL-8, and TNFα as compared to the LPS group (IL-1β 0.22-fold that of the LSP group; IL-6 0.22-fold that of the LPS group; IL-8 0.29-fold that of the LPS group; TNFα 2.30-fold that of the LPS group; $P < 0.05$; Fig. 7a–d). No significant difference was detected in the levels of inflammatory factors between the LPS group and the α7 nAChR siRNA group ($P > 0.05$). These findings indicated that the knockdown of α7 nAChR aggravated the inflammatory reaction, while agitation of α7 nAChR suppressed the inflammation in LPS-induced SH-SY5Y cells.

Discussion

Intraplantar injection of CFA in mice results in long-term mechanical allodynia and thermal hyperalgesia, which mimics injury-induced chronic inflammatory pain or infection (Bang et al. 2021; Xiang et al. 2019). Elucidating the mechanisms underlying pain hypersensitivity may identify effective therapeutic targets for treating inflammatory pain. Here, we observed that α7 nAChR is mainly localized to neurons of DRG tissues. Furthermore, CFA injection led to

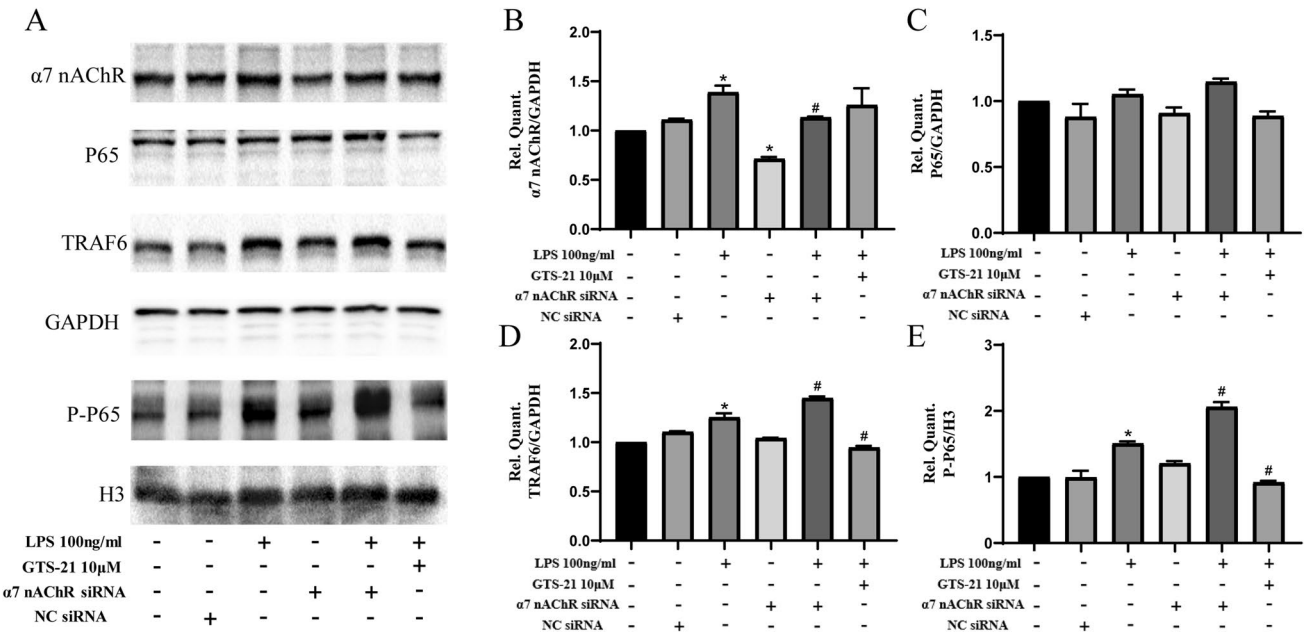

Fig. 6 Effects of α7 nAChR siRNA and GTS-21 on TRAF6/NF-κB p65 signaling pathway under inflammatory conditions induced by LPS in SH-SY5Y cells. **a** Western blot images representing α7 nAChR, P65, TRAF6, and P-P65 protein expression in neuronal SH-SY5Y cells. **b** Relative protein expression level of α7 nAChR in SH-SY5Y cells treated with LPS, α7 nAChR siRNA, LPS plus α7 nAChR siRNA, or LPS plus GTS-21. $^{*}P < 0.05$, versus NC siRNA group. One-way analysis of variance (ANOVA) followed by Bonferroni post hoc test. $^{\#}P < 0.05$, versus LPS group. **c** Relative protein expression level of P65 in SH-SY5Y cells treated with LPS, α7 nAChR siRNA, LPS plus α7 nAChR siRNA, or LPS plus GTS-21. **d** Relative protein expression level of TRAF6 in SH-SY5Y cells treated with LPS, α7 nAChR siRNA, LPS plus α7 nAChR siRNA, or LPS plus GTS-21. One-way ANOVA followed by Bonferroni post hoc test. $^{*}P < 0.05$, versus NC siRNA group, $^{\#}P < 0.05$, versus LPS group. **e** Relative protein expression level of P-P65 in SH-SY5Y cells treated with LPS, α7 nAChR siRNA, LPS plus α7 nAChR siRNA, or LPS plus GTS-21. One-way ANOVA followed by Bonferroni post hoc test. $^{*}P < 0.05$, versus NC siRNA group, $^{\#}P < 0.05$, versus LPS group

an increase in the expression level of α7 nAChR protein in the ipsilateral DRG, while inhibition of the protein expression in the injured DRGs aggravated the hyperalgesia caused by inflammatory pain. Conversely, CFA-induced mechanical and thermal pain hypersensitivities were attenuated by intrathecal α7 nAChR agonist GTS-21. Finally, we demonstrated that α7 nAChR activation suppresses the secretion of pro-inflammatory mediators in SH-SY5Y cells through the TRAF6/NF-κB P65 pathway under inflammatory conditions. These results indicated that α7 nAChR is involved in controlling the development of CFA-induced chronic inflammatory pain.

Accumulating evidence suggested that α7 nAChR is closely associated with anti-neuroinflammation through the cholinergic nervous system and serves as a molecular target for the treatment of many neurological diseases and chronic pain (Abbas et al. 2019; Bagdas et al. 2016). However, the level and distribution of α7 nAChR in DRG and the possible cellular mechanisms in modulating inflammatory pain have not yet been clearly established. Previous studies have demonstrated that α7 nAChR is upregulated under inflammatory conditions in various tissues or cell lines; thus, the elevated level of the receptor is speculated to regulate pro-inflammatory cytokine production (Khan et al. 2012; Niranjan et al. 2012; Albers et al. 2014; Bao et al. 2016; Wedn et al. 2019). For example, the α7 nAChR on macrophage-like U937 cells was reported to be upregulated after LPS stimulation (Chernyavsky et al. 2010). This is similar to studies by Bao et al., who found an increase in α7 nAChR subunit protein with LPS-stimulated placental inflammation and the receptor is considered to regulate cytokine production and leukocyte infiltration. When the inflammatory challenge is high as after LPS treatment, α7 nAChR is upregulated to assist in control of the inflammation (Bao et al. 2016). However, while inflammation is relieved by nicotine, the upregulated α7 nAChR may then decline to the normal level (Bao et al. 2016). In this study, we found that CFA injection led to a robust increase in the level of α7 nAChR in the ipsilateral L4/5 DRGs. The change in α7 nAChR was similar to the abnormal pain behavior after the CFA injection. This upregulation of α7 nAChR might compensate for the inflammatory stimulation induced by CFA injection (Bao et al. 2016).

Reportedly, the pharmacological treatment with α7 nAChR agonist produced anti-inflammatory and antinociceptive effects, whereas α7 nAChR inhibition aggravated

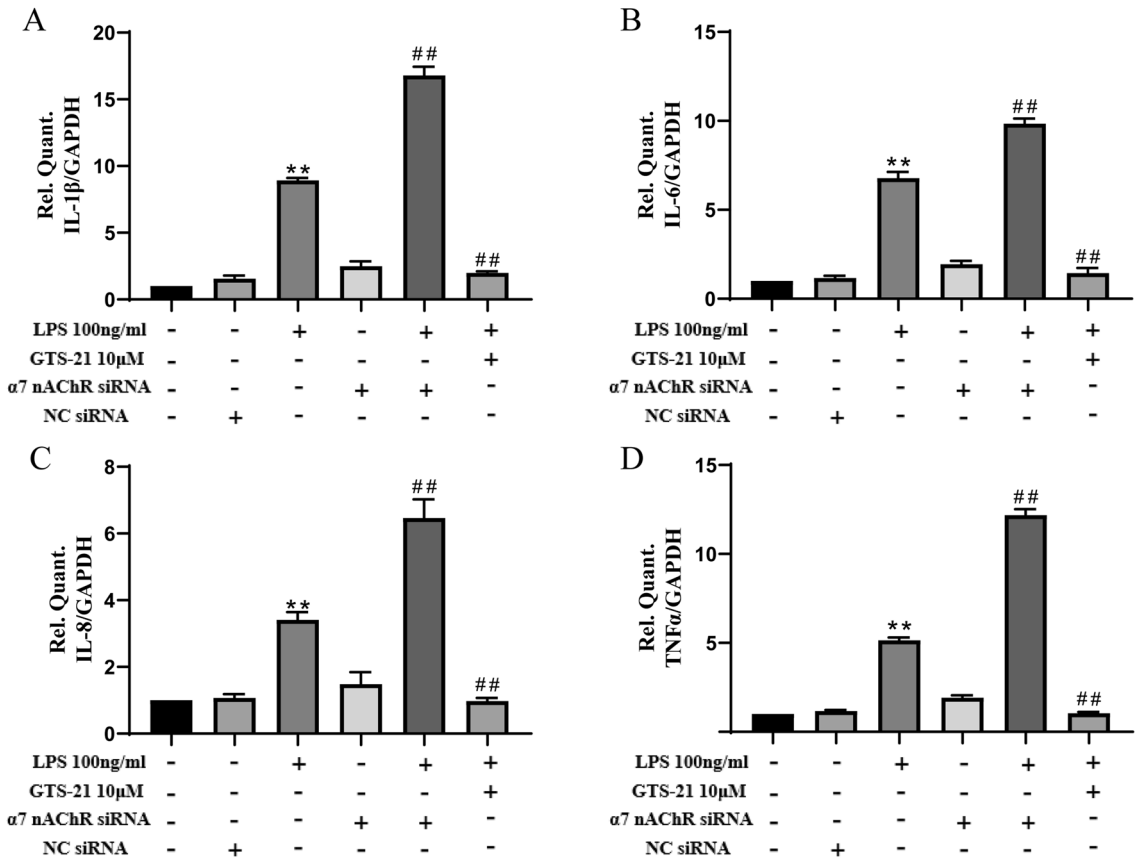

Fig. 7 Effects of α7 nAChR siRNA and GTS-21 on the release of IL-1β, IL-6, IL-8, and TNFα under inflammatory conditions induced by LPS in SH-SY5Y cells. **a**–**d** LPS stimulation increased the release of IL-1β, IL-6, IL-8, and TNFα. LPS plus α7 nAChR siRNA further aggravated the release of IL-1β, IL-6, IL-8, and TNFα compared with the LPS group. GTS-21 decreased the release of IL-1β, IL-6, IL-8, and TNFα compared with the LPS group. One-way analysis of variance (ANOVA) followed by Bonferroni post hoc test. $^{**}P < 0.01$, versus NC siRNA group, $^{\#\#}P < 0.01$, versus LPS group

the inflammatory reaction of local tissues (Khan et al. 2012). Furthermore, α7 nAChR knockout mice showed an increase in pain-related responses or resistance to the administration of α7 nAChR agonist to decrease the pain-related responses (Donvito et al. 2017; Alsharari et al. 2013). In the present study, we confirmed that microinjection of α7 nAChR siRNA in the ipsilateral L4/5 DRGs of inflammatory pain exacerbated CFA-induced pain hypersensitivity. In addition, intrathecal administration of GTS-21 alleviated the CFA-induced inflammatory pain and neuroinflammation. Taken together, these results strongly suggested that endogenous α7 nAChRs-dependent mechanisms and signaling play a role in the modification of chronic inflammatory pain-related behaviors.

The TRAF6/NF-κB signaling pathway plays a major role in the control of inflammatory responses and release of pro-inflammatory cytokines (Kim et al. 2018; Liu et al. 2020). As the upstream protein of NF-κB, TRAF6 is a key molecule in the TRAF6/NF-κB pathway (Yang et al. 2020). Additionally, it has been found that inhibition of TRAF6 downregulates the activation of NF-κB and finally alleviates the inflammatory-induced injury (Zhai et al. 2020). Similarly, the prevention of upregulated TRAF6 inhibits the expression of NF-κB (Ge et al. 2019). Intriguingly, NF-κB is a ubiquitous rapid response transcription factor that is involved in pain genesis and predominates several genes that encode nociceptive mediators, chemokines, and inflammatory cytokines (Chen et al. 2016). The intrathecal administration of the NF-κB inhibitor pyrrolidine dithiocarbamate inhibits the secretion of pro-inflammatory cytokines and improves neuropathic pain (Pinho-Ribeiro et al. 2016). Furthermore, the TRAF6/NF-κB pathway in DRG neurons is activated following peripheral nerve injury and neuroinflammation (Huang et al. 2019). This present study demonstrated that LPS triggers the expression of α7 nAChR and activates the TRAF6/NF-κB pathway in the neuronal cell line. Blocking the increased α7 nAChRs expression aggravates the upregulation of TRAF6 and NF-κB under inflammatory conditions, while agitation of α7 nAChR suppresses the activation of TRAF6/NF-κB. These results indicated that

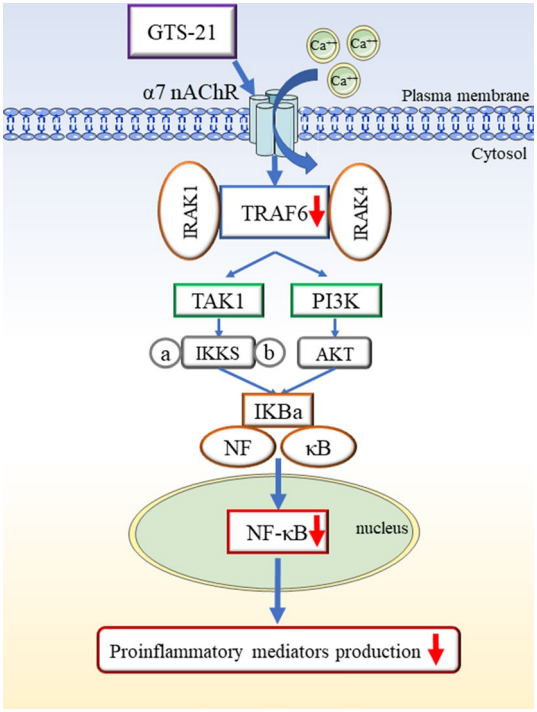

Fig. 8 Activation of α7-nAchR by GTS-21 suppresses the inflammatory response through interaction with the TRAF6/NF-κB pathway. Stimulation of α7-nAchR by GTS-21 would increase the influx of Ca^{2+}, which leads to a decrease in the expression of TRAF6, Akt, NF-κB, and pro-inflammatory mediators

the anti-inflammatory activity of α7 nAChR is mediated by blockade of the TRAF6/NF-κB signaling pathway.

Accumulating evidence indicated that neuroinflammatory response in the somatosensory pathway contributes to chronic pain from DRG to the spinal cord (Khan et al. 2016; Ortmann and Chattopadhyay 2014; Moschetti et al. 2019). Herein, we observed increased expression of IL-1β, IL-6, IL-8, and TNFα in the neuronal SH-SY5Y cells exposed to LPS, which was exacerbated by α7 nAChR siRNA treatment. However, we observed that GTS-21, a specific α7 nAChR agonist, impeded the secretion of IL-1β, IL-6, IL-8, and TNFα in SH-SY5Y cells exposed to LPS. These results agree with the findings of previous studies which showed that the absence of functional α7 nAChR declined the inhibition of the production of pro-inflammatory cytokines while agitation of α7 nAChR suppressed inflammation (Khan et al. 2012; Mengke et al. 2016), thereby providing evidence for a protective effect of α7 nAChR in diminishing neuroinflammatory response under inflammatory conditions.

Conclusions

This study assessed α7 nAChR expression and distribution in DRG neurons and determined their protective function in CFA-induced pain hypersensitivity. The underlying mechanism might involve suppressing the TRAF6/NF-κB activation and inhibiting the pro-inflammatory cytokine expression by α7 nAChR agitation. These findings imply that α7 nAChR may be potentially used as a therapeutic target for preventing and treating chronic pain. Activation of α7-nAChR by GTS-21 suppresses the inflammatory response through interaction with the TRAF6/NF-κB pathway as illustrated in Fig. 8.

Supplementary Information The online version contains supplementary material available at https://doi.org/10.1007/s10787-021-00873-0.

Author contributions (I) Conception and design: XZ, LH; (II) Administrative support: JL, LH; (III) Provision of study materials or patients: all authors; (IV) Collection and assembly of data: all authors; (V) Data analysis and interpretation: all authors; (VI) Manuscript writing: all authors; (VII) Final approval of manuscript: all authors.

Funding This study was supported by the National Natural Science Foundation of China (No. 81401576); Shanghai Municipal Commission of Health and Family Planning, China (No. 20164Y0263). The authors would like to express their gratitude to EditSprings (https://www.editsprings.com/) for the expert linguistic services provided.

Declarations

Conflict of interest The authors have no conflicts of interest to declare.

Ethical statement The authors are accountable for all aspects of the work in ensuring that questions related to the accuracy or integrity of any part of the work are appropriately investigated and resolved. The animal experiments were approved by the Laboratory Animal Ethics Committee of International Peace Maternity & Child Health Hospital (Shanghai, China).

References

Abbas M, Alzarea S, Papke RL, Rahman S (2019) The α7 nicotinic acetylcholine receptor positive allosteric modulator prevents lipopolysaccharide-induced allodynia, hyperalgesia and TNF-α in the hippocampus in mice. Pharmacol Rep 71:1168–1176

Albers KM, Zhang XL, Diges CM, Schwartz ES, Yang CI, Davis BM, Gold MS (2014) Artemin growth factor increases nicotinic cholinergic receptor subunit expression and activity in nociceptive sensory neurons. Mol Pain 10:31

Alsharari SD, Freitas K, Damaj MI (2013) Functional role of alpha7 nicotinic receptor in chronic neuropathic and inflammatory pain: studies in transgenic mice. Biochem Pharmacol 86:1201–1207

Bagdas D, Wilkerson JL, Kulkarni A, Toma W, Alsharari S, Gul Z, Lichtman AH, Papke RL, Thakur GA, Damaj MI (2016) The α7 nicotinic receptor dual allosteric agonist and positive allosteric modulator GAT107 reverses nociception in mouse models of inflammatory and neuropathic pain. Br J Pharmacol 173:2506–2520

Bagdas D, Gurun MS, Flood P, Papke RL, Damaj MI (2018) New insights on neuronal nicotinic acetylcholine receptors as targets for pain and inflammation: a focus on α7 nAChRs. Curr Neuropharmacol 16:415–425

Bang S, Donnelly CR, Luo X, Toro-Moreno M, Tao X, Wang Z, Chandra S, Bortsov AV, Derbyshire ER, Ji RR (2021) Activation of GPR37 in macrophages confers protection against infection-induced sepsis and pain-like behaviour in mice. Nat Commun 12:1704

Bao J, Liu Y, Yang J, Gao Q, Shi SQ, Garfield RE, Liu H (2016) Nicotine inhibits LPS-induced cytokine production and leukocyte infiltration in rat placenta. Placenta 39:77–83

Baron EP, Lucas P, Eades J, Hogue O (2018) Patterns of medicinal cannabis use, strain analysis, and substitution effect among patients with migraine, headache, arthritis, and chronic pain in a medicinal cannabis cohort. J Headache Pain 19:37

Busse JW, Wang L, Kamaleldin M, Craigie S, Riva JJ, Montoya L, Mulla SM, Lopes LC, Vogel N, Chen E, Kirmayr K, de Oliveira K, Olivieri L, Kaushal A, Chaparro LE, Oyberman I, Agarwal A, Couban R, Tsoi L, Lam T, Vandvik PO, Hsu S, Bala MM, Schandelmaier S, Scheidecker A, Ebrahim S, Ashoorion V, Rehman Y, Hong PJ, Ross S, Johnston BC, Kunz R, Sun X, Buckley N, Sessler DI, Guyatt GH (2018) Opioids for chronic noncancer pain: a systematic review and meta-analysis. JAMA 320:2448–2460

Chen Y, Chen X, Yu J, Xu X, Wei X, Gu X, Liu C, Zhang D, Xu Z (2016) JAB1 is involved in neuropathic pain by regulating JNK and NF-κB activation after chronic constriction injury. Neurochem Res 41:1119–1129

Chernyavsky AI, Arredondo J, Skok M, Grando SA (2010) Auto/paracrine control of inflammatory cytokines by acetylcholine in macrophage-like U937 cells through nicotinic receptors. Int Immunopharmacol 10:308–315

Chrestia JF, Bruzzone A, Esandi MDC, Bouzat C (2021) Tyrosine phosphorylation differentially fine-tunes ionotropic and metabotropic responses of human α7 nicotinic acetylcholine receptor. Cell Mol Life Sci 78:5381–5395

Criscuolo C, Accorroni A, Domenici L, Origlia N (2015) Impaired synaptic plasticity in the visual cortex of mice lacking α7-nicotinic receptor subunit. Neuroscience 294:166–171

Debar L, Benes L, Bonifay A, Deyo RA, Elder CR, Keefe FJ, Leo MC, McMullen C, Mayhew M, Owen-Smith A, Smith DH, Trinacty CM, Vollmer WM (2018) Interdisciplinary team-based care for patients with chronic pain on long-term opioid treatment in primary care (PPACT)—protocol for a pragmatic cluster randomized trial. Contemp Clin Trials 67:91–99

Donvito G, Bagdas D, Toma W, Rahimpour E, Jackson A, Meade JA, Alsharari S, Kulkarni AR, Ivy Carroll F, Lichtman AH, Papke RL, Thakur GA, Imad Damaj M (2017) The interaction between alpha 7 nicotinic acetylcholine receptor and nuclear peroxisome proliferator-activated receptor-α represents a new antinociceptive signaling pathway in mice. Exp Neurol 295:194–201

Ge YT, Zhong AQ, Xu GF, Lu Y (2019) Resveratrol protects BV2 mouse microglial cells against LPS-induced inflammatory injury by altering the miR-146a-5p/TRAF6/NF-κB axis. Immunopharmacol Immunotoxicol 41:549–557

Ghasemlou N, Chiu IM, Julien JP, Woolf CJ (2015) CD11b+Ly6G- myeloid cells mediate mechanical inflammatory pain hypersensitivity. Proc Natl Acad Sci USA 112:E6808–E6817

Godin JR, Roy P, Quadri M, Bagdas D, Toma W, Narendrula-Kotha R, Kishta OA, Damaj MI, Horenstein NA, Papke RL, Simard AR (2019) A silent agonist of α7 nicotinic acetylcholine receptors modulates inflammation ex vivo and attenuates EAE. Brain Behav Immun 87:286–300

Huang LN, Zou Y, Wu SG, Zhang HH, Mao QX, Li JB, Tao YX (2019) Fn14 participates in neuropathic pain through NF-κB pathway in primary sensory neurons. Mol Neurobiol 56:7085–7096

Kalkman HO, Feuerbach D (2016) Modulatory effects of α7 nAChRs on the immune system and its relevance for CNS disorders. Cell Mol Life Sci 73:2511–2530

Khan MA, Farkhondeh M, Crombie J, Jacobson L, Kaneki M, Martyn JA (2012) Lipopolysaccharide upregulates α7 acetylcholine receptors: stimulation with GTS-21 mitigates growth arrest of macrophages and improves survival in burned mice. Shock 38:213–219

Khan S, Choi RJ, Lee J, Kim YS (2016) Attenuation of neuropathic pain and neuroinflammatory responses by a pyranocoumarin derivative, anomalin in animal and cellular models. Eur J Pharmacol 774:95–104

Kim B, Lee KY, Park B (2018) Icariin abrogates osteoclast formation through the regulation of the RANKL-mediated TRAF6/NF-κB/ERK signaling pathway in Raw264.7 cells. Phytomedicine 51:181–190

Liang L, Fan L, Tao B, Yaster M, Tao YX (2013) Protein kinase B/Akt is required for complete Freund's adjuvant-induced upregulation of Nav1.7 and Nav1.8 in primary sensory neurons. J Pain 14:638–647

Licheri V, Lagstr MO, Lotfi A, Patton MH, Wigstr MH, Mathur B, Adermark L (2018) Complex control of striatal neurotransmission by nicotinic acetylcholine receptors via excitatory inputs onto medium spiny neurons. J Neurosci 38:6597–6607

Liu GJ, Zhang QR, Gao X, Wang H, Tao T, Gao YY, Zhou Y, Chen XX, Li W, Hang CH (2020) MiR-146a ameliorates hemoglobin-induced microglial inflammatory response via TLR4/IRAK1/TRAF6 associated pathways. Front Neurosci 14:311

Loram LC, Harrison JA, Chao L, Taylor FR, Reddy A, Travis CL, Giffard R, Al-Abed Y, Tracey K, Maier SF, Watkins LR (2010) Intrathecal injection of an alpha seven nicotinic acetylcholine receptor agonist attenuates gp120-induced mechanical allodynia and spinal pro-inflammatory cytokine profiles in rats. Brain Behav Immun 24:959–967

Maiar M, Leese C, Certo M, Echeverria-Altuna I, Mangione AS, Arsenault J, Davletov B, Hunt SP (2018) Selective neuronal silencing using synthetic botulinum molecules alleviates chronic pain in mice. Sci Transl Med 10:eaar7384

Matsuoka Y, Yamashita A, Matsuda M, Kawai K, Sawa T, Amaya F (2019) NLRP2 inflammasome in dorsal root ganglion as a novel molecular platform that produces inflammatory pain hypersensitivity. Pain 160:2149–2160

Mengke NS, Hu B, Han QP, Deng YY, Fang M, Xie D, Li A, Zeng HK (2016) Rapamycin inhibits lipopolysaccharide-induced neuroinflammation in vitro and in vivo. Mol Med Rep 14:4957–4966

Moschetti G, Amodeo G, Paladini MS, Molteni R, Balboni G, Panerai A, Sacerdote P, Franchi S (2019) Prokineticin 2 promotes and sustains neuroinflammation in vincristine treated mice: focus on pain and emotional like behavior. Brain Behav Immun 82:422–431

Müller-Schwefe G, Morlion B, Ahlbeck K, Alon E, Coaccioli S, Coluzzi F, Huygen F, Jaksch W, Kalso E, Kocot-Kępska M, Kress HG, Mangas AC, Margarit Ferri C, Mavrocordatos P, Nicolaou A, Hernández CP, Pergolizzi J, Schäfer M, Sichère P (2017) Treatment for chronic low back pain: the focus should change to multimodal management that reflects the underlying pain mechanisms. Curr Med Res Opin 33:1199–1210

Niranjan R, Nath C, Shukla R (2012) Melatonin attenuated mediators of neuroinflammation and alpha-7 nicotinic acetylcholine receptor mRNA expression in lipopolysaccharide (LPS) stimulated rat astrocytoma cells, C6. Free Radic Res 46:1167–1177

Ortmann KL, Chattopadhyay M (2014) Decrease in neuroimmune activation by HSV-mediated gene transfer of TNFα soluble receptor

alleviates pain in rats with diabetic neuropathy. Brain Behav Immun 41:144–151

Pasquale MK, Dufour R, Schaaf D, Reiners AT, Mardekian J, Joshi AV, Patel NC (2014) Pain conditions ranked by healthcare costs for members of a national health plan. Pain Pract 14:117–131

Peng H, Zou L, Xie J, Wu H, Wu B, Zhu G, Lv Q, Zhang X, Liu S, Li G, Xu H, Gao Y, Xu C, Zhang C, Wang S, Xue Y, Liang S (2017) lncRNA NONRATT021972 siRNA decreases diabetic neuropathic pain mediated by the P2X(3) receptor in dorsal root ganglia. Mol Neurobiol 54:511–523

Pinho-Ribeiro FA, Fattori V, Zarpelon AC, Borghi SM, Staurengo-Ferrari L, Carvalho TT, Alves-Filho JC, Cunha FQ, Cunha TM, Casagrande R, Verri WA (2016) Pyrrolidine dithiocarbamate inhibits superoxide anion-induced pain and inflammation in the paw skin and spinal cord by targeting NF-κB and oxidative stress. Inflammopharmacology 24:97–107

Ruan X, Kaye AD (2016) A call for saving interdisciplinary pain management. J Orthop Sports Phys Ther 46:1021–1023

Sabec MH, Wonnacott S, Warburton EC, Bashir ZI (2018) Nicotinic acetylcholine receptors control encoding and retrieval of associative recognition memory through plasticity in the medial prefrontal cortex. Cell Rep 22:3409–3415

Shenkarev ZO, Shulepko MA, Bychkov ML, Kulbatskii DS, Shlepova OV, Vasilyeva NA, Andreev-Andrievskiy AA, Popova AS, Lagereva EA, Loktyushov EV, Koshelev SG, Thomsen MS, Dolgikh DA, Kozlov SA, Balaban PM, Kirpichnikov MP, Lyukmanova EN (2020) Water-soluble variant of human Lynx1 positively modulates synaptic plasticity and ameliorates cognitive impairment associated with α7-nAChR dysfunction. J Neurochem 155:45–61

Stötzner P, Spahn V, Celik M, Labuz D, Machelska H (2018) Mu-opioid receptor agonist induces Kir3 currents in mouse peripheral sensory neurons—effects of nerve injury. Front Pharmacol 9:1478

Sun R, Liu Y, Hou B, Lei Y, Bo J, Zhang W, Sun Y, Zhang Y, Zhang Z, Liu Z, Huo W, Mao Y, Ma Z, Gu X (2019) Perioperative activation of spinal α7 nAChR promotes recovery from preoperative stress-induced prolongation of postsurgical pain. Brain Behav Immun 79:294–308

van Hecke O, Austin SK, Khan RA, Smith BH, Torrance N (2014) Neuropathic pain in the general population: a systematic review of epidemiological studies. Pain 155:654–662

Wedn AM, El-Gowilly SM, El-Mas MM (2019) Nicotine reverses the enhanced renal vasodilator capacity in endotoxic rats: role of α7/α4β2 nAChRs and HSP70. Pharmacol Rep 71:782–793

Xiang X, Wang S, Shao F, Fang J, Xu Y, Wang W, Sun H, Liu X, Du J (2019) Electroacupuncture stimulation alleviates CFA-induced inflammatory pain via suppressing P2X3 expression. Int J Mol Sci 20:3248

Yang Y, Tan X, Xu J, Wang T, Liang T, Xu X, Ma C, Xu Z, Wang W, Li H, Shen H, Li X, Dong W, Chen G (2020) Luteolin alleviates neuroinflammation via downregulating the TLR4/TRAF6/NF-κB pathway after intracerebral hemorrhage. Biomed Pharmacother 126:110044

Zhai X, Yan Z, Zhao J, Chen K, Yang Y, Cai M, He C, Huang C, Li B, Yang M, Zhou X, Zhao Y, Wei X, Bai Y, Li M (2020) Muscone ameliorates ovariectomy-induced bone loss and receptor activator of nuclear factor-κb ligand-induced osteoclastogenesis by suppressing TNF receptor-associated factor 6-mediated signaling pathways. Front Pharmacol 11:348

Zhao JY, Liang L, Gu X, Li Z, Wu S, Sun L, Atianjoh FE, Feng J, Mo K, Jia S, Lutz BM, Bekker A, Nestler EJ, Tao YX (2017) DNA methyltransferase DNMT3a contributes to neuropathic pain by repressing Kcna2 in primary afferent neurons. Nat Commun 8:14712